BULLETIN OF THE POLISH ACADEMY OF SCIENCES
TECHNICAL SCIENCES
Vol. 55, No. 2, 2007

Fabrication and characterization of 1-D alumina (Al_2O_3) nanofibers in an electric field

A.-M. AZAD*, M. NOIBI, and M. RAMACHANDRAN

Department of Chemical and Environmental Engineering, The University of Toledo, 3052 Nitschke Hall, 2801 W. Bancroft St., Toledo, OH 43606-3390, USA

Abstract. The technique of electrospinning was employed to fabricate uniform one-dimensional inorganic-organic composite nanofibers at room temperature from a solution containing equal volumes of aluminum 2, 4-pentanedionate in acetone and polyvinylpyrrolidone in ethanol. Upon firing and sintering under carefully pre-selected time-temperature profiles (heating rate, temperature and soak time), high-purity and crystalline alumina nanofibers retaining the original morphological features present in the as-spun composite (cermer) fibers were obtained. Tools such as laser Raman spectroscopy, scanning and transmission electron microscopy together with energy dispersive spectroscopy and selected area electron diffraction were employed to follow the systematic evolution of the ceramic phase and its morphological features in the as-spun and the fired fibers. X-ray diffraction was used to identify the crystalline fate of the final product.

Key words: electrospinning, alumina nanofibers, electron microscopy, Raman spectroscopy, X-ray diffraction.

1. Introduction

Recently, for the fabrication of nanostructures bottom-up approaches have received increasing attention and electrospinning (e-spinning) is one of them. The technique of e-spinning was discovered nearly 100 years ago [1] and has been successfully used for making polymer nanofibers for the past several decades [2–12]; the first US patent was issued in 1934 [13]. As is well known, the technique of electrospinning uses external electrical forces to produce novel polymeric fibers of diameters in the range of 3–1000 nm, depending upon the strength of the applied voltage between a drop of the precursor solution (or melt) and the collecting surface. Electrospinning occurs when the electrical forces at the surface of the drop overcome the surface tension. When this happens, the solution or melt is ejected as an electrically charged jet and shoots towards the oppositely charged electrode. Upon reaching the collector surface, it gets neutralized and collects as dry nanofibers. Figure 1 shows the basic set-up and working principle of this technique [14].

The possibility of extending the concept to ceramic systems has opened a new era in nanoscale research during the past couple of years. It is possible to synthesize these one-dimensional nanofibers in pure form or as suitable ceramic-polymer composites. It is also envisaged that by controlling the jet orifice, one can control the diameter of the resulting nanofibrillar structures, thereby modifying their key properties such as structure, elasticity, strength and resistance to fracture, thermal and electrical conductivity, and optical characteristics, etc. [15–17]. Thus, it has seen a revival and its adaptation to ceramic systems. Several papers and patents have since been published and issued [16–23]. Sigmund et al. have recently reviewed the processing and structure relationships in the electrospun ceramic fibers [24]. Potential application of this technology includes biological membranes for immobilized enzymes and catalysts, artificial blood vessels, anti-septic wound dressing materials, aerosol filters, to name a few. The possibility of extending the concept to ceramic systems would open a new era in nanoscale research. Examples of such novel nanocomposites would be: piezoelectric-polymers, magnetic-polymers or optical polymers, depending upon the choice of the ceramic component of the composite. Furthermore, by establishing adequate processing protocols, it is possible to form a nanofiber composite of two ceramics in a core-shell concentric design [9,25]. Such nanocomposites would find immense applications as lightweight, inexpensive, high-strength structural as well as multifunctional components. By using an orthogonal set up (electrospinning simultaneously at right-angles), a matty design of a given ceramic or two ceramic nanofibers can also be fabricated; a possible application of such a design would be the clothing membranes for protection against fire, battlefield threat and environmental hazards.

Alumina (Al_2O_3) is a well-known material among functional ceramics – in the area of catalysis, microelectronics and optics [26–27] – both in pure form as well as in combination with others. Its applications range from pure and transparent thin films as optical windows to particulates, platelets and fibers as strengthening reinforcements in light-weight ultra-strong metal matrix composites. Giving due cognizance to the potential application of

*e-mail: abdul-majeed.azad@utoledo.edu

ceramic nanofibers in general and of alumina nanofibers in particulars, we report in this communication the fabrication, processing and characterization of transparent one-dimensional alumina nanofibers via e-spinning. In the present work, target composition was first electrospun in the form of ceramic-polymer ('cermer') composite fibers from a suitable homogeneous mixture of a simple aluminum precursor solution and a polymer. The as-spun fibers were subsequently processed to yield the desired alumina ceramic. The transformation of cermer to ceramic was followed by a series of heat-treatment and the systematic phase evolution. The morphological features of the products subsequent to each of such heat-treatments were verified by laser Raman spectroscopy (LRS), X-ray diffraction (XRD), scanning electron microscopy coupled with energy dispersive spectroscopy (SEM-EDS) and transmission electron microscopy coupled with energy dispersive spectroscopy and selected area electron diffraction (TEM-EDS-SAED) techniques.

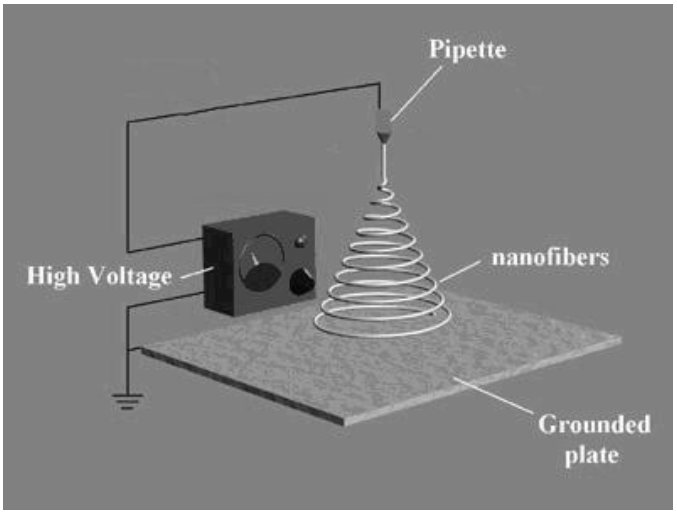

Fig. 1. An illustrative schematic of the electrospinning process after Ref. 14

2. Experimental procedure

High-purity aluminum 2, 4-pentanedionate $[Al(CH_3COCHCOCH_3)_3]$ from Alfa-Aesar, MA, USA (purity 99.995%) was used as the precursor for the synthesis of alumina fibers. Adequate amount of the white crystalline powder was dissolved in ACS grade acetone (Alfa-Aesar, 99.5% +) by gentle stirring until clear. Typical concentration of the aluminum pentanedionate solution (AP) used in this work was $\sim 6.85 \times 10^{-2}$ mol L^{-1}. Granular polyvinyl pyrrolidone (PVP, average molecular weight $\sim 1.3 \times 10^6$, Alfa-Aesar, MA, USA) was used as the polymeric component of all the composites fabricated in this study. The polymeric solution was made by dissolving the PVP granular powder in reagent grade ethanol (Fisher Chemicals, PA, USA) under constant and vigorous stirring to give 15 wt. % PVP solution. This concentration was arrived at and selected after several preliminary iterations with respect to the desired viscosity of the inorganic-organic composite solutions were carried out. Due to pronounced volatility of ethanol during and after the preparation, the PVP solution was prepared only when electrospinning was to be carried out; PVP solutions tended to dry out and leave a stiff gel in the container upon prolonged storage. However, the aluminum precursor solution in acetone could stay clear and last for much longer duration without forming any sol; it did not require any stabilization either.

For the electrospinning experiments, equal volumes of the precursor solutions (AP and PVP) were added to a beaker and thoroughly mixed with the aid of a magnetic stirrer to form a homogeneous viscous solution. After mixing, this solution was drawn into a 5 ml capacity Benton-Dickinson clinical syringe (VWR International, IL, USA). Precision-tip 1.5 in. long 23 gauge stainless steel needles (from EFD Inc., RI, USA) were attached to the syringe, which was mounted on a programmable syringe pump (KDS-100). The syringe and needle make and type, flow rate and amount to dispense were entered in the syringe pump memory through the front panel. The pump could be operated either in horizontal or vertical configuration and no difference was noted in the quality of the fibers thus produced. The preferred orientation of the syringe pump in this work was horizontal. A DC power supply using the high voltage system from Ultra Volt (NP-30; rated for 30 kV/4W; HNY, USA) and a circuit design originally developed at NASA Glenn Research Center [28] was fabricated in-house and used in this work for electrospinning. The circuit allows the application of a steady dc voltage in a gradual fashion between the fluid droplet and the neutralizer. One (negative) terminal of the power supply was connected to the needle, while the other (positive) was connected to the grounded collector plate.

In order to enhance the fiber collection area a modified design of collector plates were used. Previously, we have used a collector plate made by layering several thicknesses of aluminum foil into approximately, a 4×4 in. square; for the ease of sample handling and subsequently processing, ceramic dishes/plates were used to collect the fibers where a small 1×1 in. aluminum foil was attached to the back of the dish with double-sided tape and the electrode was hooked to the foil [29,30]. This allowed the fibers to be collected directly onto the ceramic plate. In the present work, a pair two stainless steel plates (4×4 in.) instead of one was employed. The plates were connected together to a common junction by soldering short lengths of electrical lead wires to the center of each plate at the back, and were place next to each other about an inch apart. This allowed the fibers to spread across the plates including the empty region between them. In order to minimize the electrostatic/ electromagnetic induction effects, the use of metallic components in the vicinity of the e-spinning set-up was totally eliminated by supporting the collector plates against a wooden stand that was held in a porcelain base. Schematic of the modified collector plate design in shown in Fig. 2.

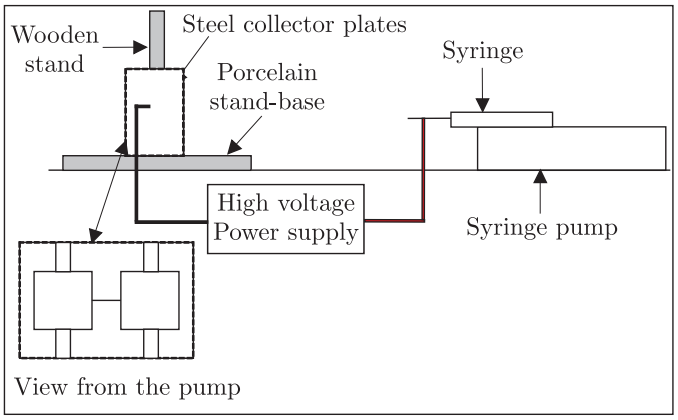

Fig. 2. A modified system of fiber collection adopted in this work

Using the power supply, a voltage of 7–9 kV was applied between the needle and the collectors in order to initiate the e-spinning. After the voltage was turned on, the syringe pump was started. The voltage was tweaked precisely by adjusting the voltage knob in small steps in both the directions until the fibers began to form steadily and collect on the plates placed about 4 in. away from the tip of the needle. A flow rate of 0.03 ml/h was chosen and the cermer fibers were spun continuously with short intermittent interruptions (lasting about 5 sec.) of the run for the cleaning of clogged needle-tip from time to time. The process variables were optimized after considerable simulation and several preliminary experiments. On an average, it took about 800h to spin $\sim$ 10 ml of the composite solution. Under optimized processing conditions, continuous and long fibers spun uniformly and collected in the form of non-woven mat, which increased in volume with time.

After spinning was complete, small amounts of the as-spun composite fibers were used for characterization by Raman spectroscopy and scanning electron microscopy. The remaining fibers were collected on zirconia crucibles and fired at 1000, 1300 and 1500°C for 1h in two stages. In order to retain these fibrillar artifacts in the processed ceramic as well, firing in a carefully selected heating and cooling profile is warranted. Various batches of dry cermer fibers were first heated slowly at a ramp rate of $1/2°$ min.$^{-1}$ up to 500°C (soak time, 1h) followed by a second firing up to 1000, 1300 or 1500°C for 1h at the same heating rate of $1/2°$ min.$^{-1}$. The second stage heat-treatment is meant to facilitate crystallization and consolidation of the desired ceramic phase. The small heating rates were chosen so as to ensure the removal of organic components without destroying the nanofibrillar morphological features in the end product and also to avoid the disintegration of the alumina fibers; it is well known that alumina exhibits rather poor thermal shock resistance, even in bulk. Fired samples were characterized by a host of analytical techniques, such as, Raman spectroscopy, X-ray diffraction, scanning and transmission electron microscopy, energy dispersive spectroscopy and selected area diffraction.

3. Results and discussion

Figure 3 shows Al_2O_3-PVP composite fibers formed in real-time on and between the twin collector plates with a taut cloth-like distribution, which could be peeled off rather easily for further processing, while Fig. 4 shows the scanning electron micrographs (acquired on a Philips XL30 FEG SEM) of the same. Individual fibers possessing uniform morphological features with large aspect ratio can be easily seen. Directionality endowed to the as-spun fibers under the influence of the imposed electric field is also evident.

Fig. 3. Collection of the wafer-like non-woven mat of the as-spun Al_2O_3-PVP composite

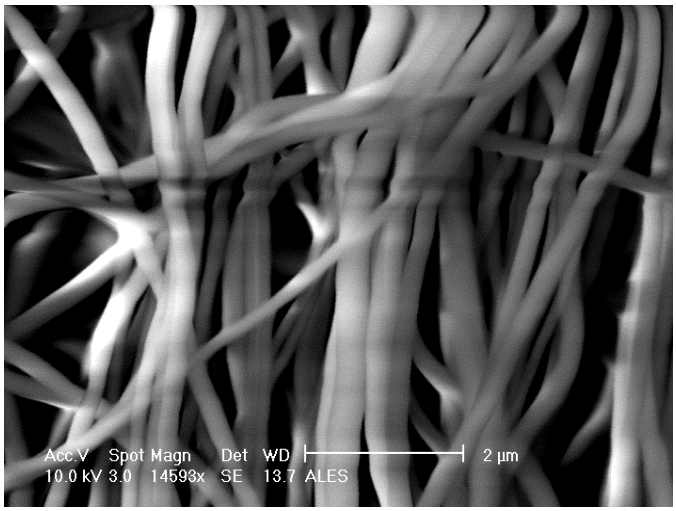

Fig. 4. Morphological features of the as-spun AP-PVP fibers

The SEM pictures of the composite fibers fired in static air environment for 1h each at 1000 and 1300°C are shown in Figure 5 and 6, respectively. As can be readily seen, the fibrillar attributes observed in the as-spun composite are fully retained in the fired samples, with the expected and considerable decrease in the fiber diameter.

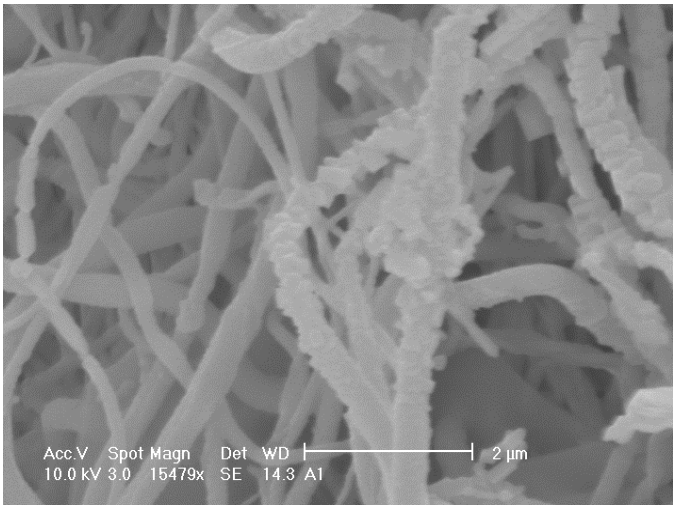

Fig. 5. SEM image of the fibers calcined at 1000°C/1h; the fibrillar features are retained in the fired ceramic after the polymer has been removed

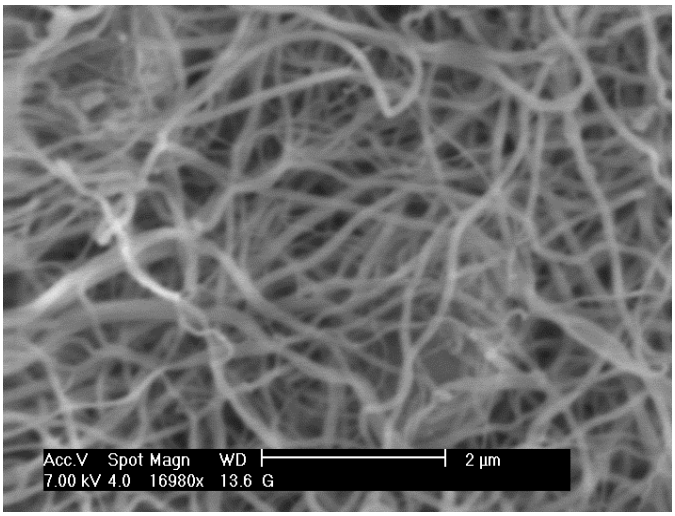

Fig. 6. SEM image of the fibers from composite calcined at 1300°C/1h

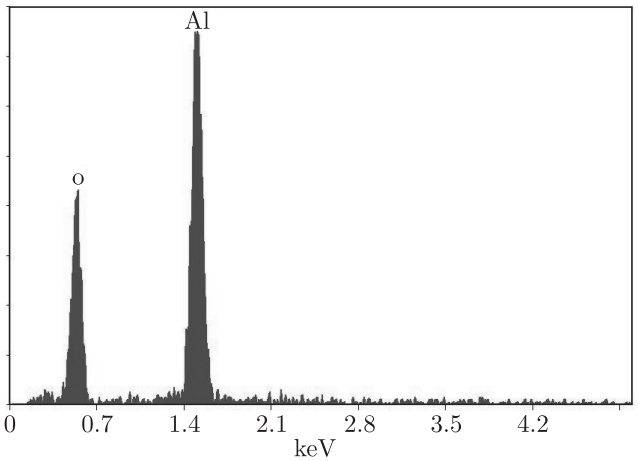

Fig. 7. EDS signature in the Al_2O_3 fibers fired at 1000°C for 1h

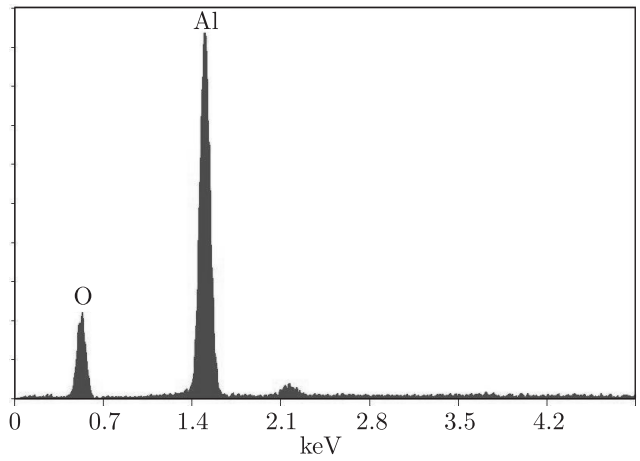

Fig. 8. The energy dispersive spectrum (EDS) of the fibers fired at 1500°C/1h

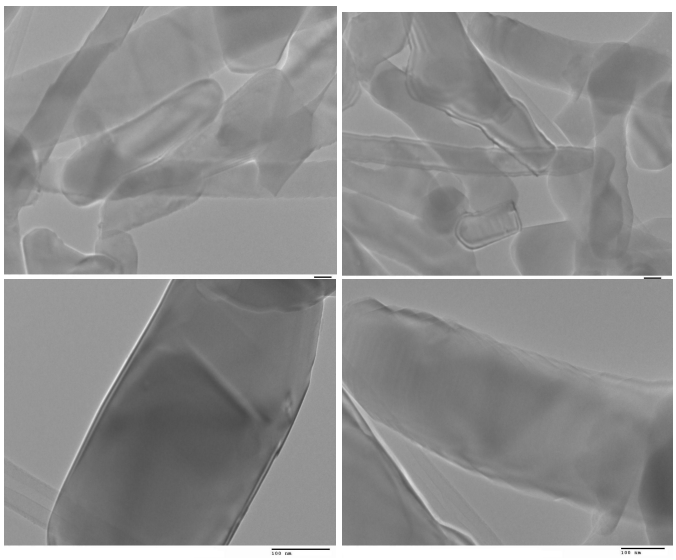

Fig. 9. TEM images of the electrospun fibers fired at 1500°C/1h (bar = 100 nm)

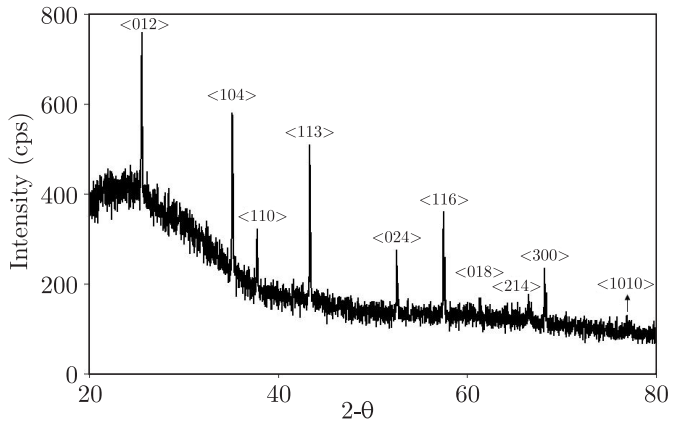

Fig. 10. XRD signature of the electrospun Al_2O_3 fibers fired at 1500°C for 1 h

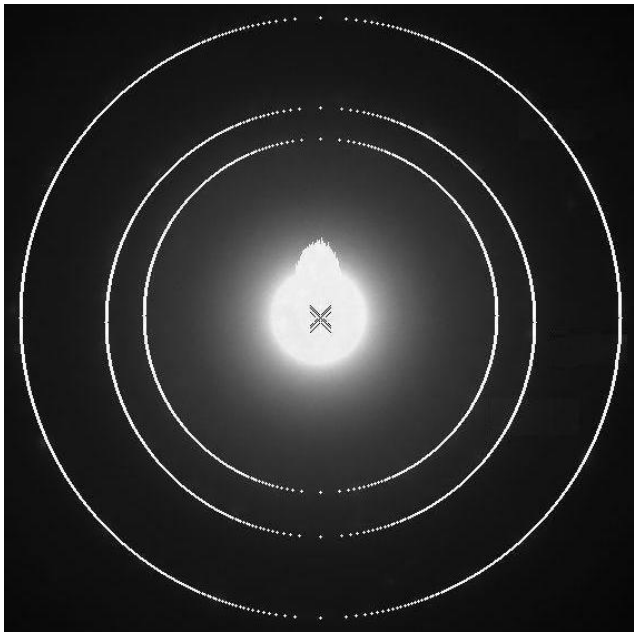

Fig. 11. SAED pattern of the electrospun fibers fired at 1500°C for 1 h

It is also interesting to note that as the calcination temperature increased further, grain coalescence, intergranular connectivity and interfibrillar cross-linking became increasing evident. The energy dispersive spectra acquired on the fibers fired at 1000°C for 1h, shown in Fig. 7 indicate the presence of aluminum and oxygen alone. The elemental quantification (within the (3% permissible error limit) performed by the standardless ZAF correction method yields the average aluminum concentration to be 43.76 wt. % (31.57 at. %) which is rather in large deviation from 52.93 wt. %, had the product been stoichiometric alumina (Al_2O_3) after this heat-treatment.

It is well known that the formation and crystallization of aluminum oxide goes through a number of phase transition schemes, one of which involves the formation of boehmite phase, AlO(OH), particularly in the case of aluminum hydroxide or other complex precursors. The most accepted pathway of dehydration followed by several sequential transitions from a polymeric, partially disordered state to the crystalline α-alumina via a number of intermediates can be represented as [31,32]:
AlO(OH) (Boehmite) $\rightarrow$ γ-Al_2O_3 $\rightarrow$ δ-Al_2O_3 $\rightarrow$ θ-Al_2O_3 $\rightarrow$ α-Al_2O_3.

The theoretical weight fraction of aluminum in boehmite is 45%, which is in good agreement with that obtained from the EDS analysis of the fibers fired at 1000°C. Thus, it is likely that at this stage, the aluminum precursor in the AP-PVP composite is reduced to boehmite instead of the target phase, alumina.

On the other hand, the quantitative analysis of the EDS spectrum (shown in Fig. 8) of the fibers obtained after they were calcined at 1500°C for 1h yielded a value of 54.84 wt. % aluminum in the calcined fibers, thereby confirming that fibers are indeed those of alumina.

At this juncture, it is natural to speculate the presence of carbon as an impurity in the fired samples resulting from the degradation and carburization of PVP upon heat-treatment of the as-spun composite fibers. It is, however, rather hard to detect carbon if formed, by XRD, especially if it is present as trace impurity, but it is possible to identify it easily by Raman spectroscopy since carbon is strongly Raman active. The distinct D and G peaks of carbon are observed around 1332–1350 and 1560–1600 cm^{-1}, respectively [33–35]. The laser Raman spectroscopy (LSR) data collected in the wave numbers range of 1200 to 2000 cm^{-1} (LabRam, Jobin-Yvon Horiba Inc., laser excitation wavelength = 633 nm) showed no Raman signal characteristic of D or G peak for carbon in the spectrum collected on the fibers fired at 1500°C for 1h. Thus, the carbon from the polymeric component as well as from the organic precursor of aluminum is completely eliminated during the heat-treatment adopted here. Furthermore, the Raman peaks of the fired fibers were found to be identical to those obtained on commercial α-alumina powder, and are well documented for the Al-O bonds in alumina specimen [37].

The transmission electron micrographs of the composite fired at 1500°C are shown in Fig. 9; on average the fibers are $\sim$ 150 nm across the diameter and are transparent. The quantitative analysis of the TEM-EDS spectrum of these fibers yielded a value of 56.4 wt.% aluminum in the calcined fibers, thereby confirming that fibers are indeed those of alumina.

Figure 10 shows the room temperature XRD pattern (Philips, PW 3050/60 X'pert Pro) of the fibers fired at 1500°C, which conforms to that of α-alumina (ICDD card # 74-0323). The selected area electron diffraction (SAED) pattern shown in Fig. 11 also confirmed the evolved phase to be α-alumina.

The XRD data was also used to compute the approximate crystallite size in the using Scherrer equation [38–40] that relates the full-width of the most intense peak at the center of the maximum height (FWHM) and the diffraction angle as follows:

$$s = \frac{K\lambda}{\beta_{1/2}\cos\theta}$$

where s is the crystallite size (Å), λ, the wave length of the incident radiations, $\beta_{1/2}$, the FWHM of the Bragg peak, θ is the Bragg angle of diffraction of the selected peak; K is the Scherrer constant whose value varies between 0.9 and 1.2 depending upon the shape of the particle under consideration (spherical, cubic or otherwise) [41–43]; we used a value of 0.94 for K [36] in the Scherrer equation for the two most intense diffractions, viz., <104> and <113>, which yielded 2.5 nm as an average value for the crystallite size in the alumina fibers calcined at 1500°C. The TEM picture of the debris of the same fibers (Fig. 12) shows alumina grains to be in the size range of 3–5 nm; this is in contrast to the grain size up to 60 nm and 110 nm in the alumina-borate fibers calcined for 2h at 1000 and

1200°C, respectively, reported by Dai et al. [44]. A high resolution TEM image of the alumina nanofibers shown in Fig. 13 yielded a value of d-spacing = 0.3484 nm, which agrees very well with the value of 0.348 nm for the diffraction in the <012> plane reported for corundum alumina (ICCD 42-1468).

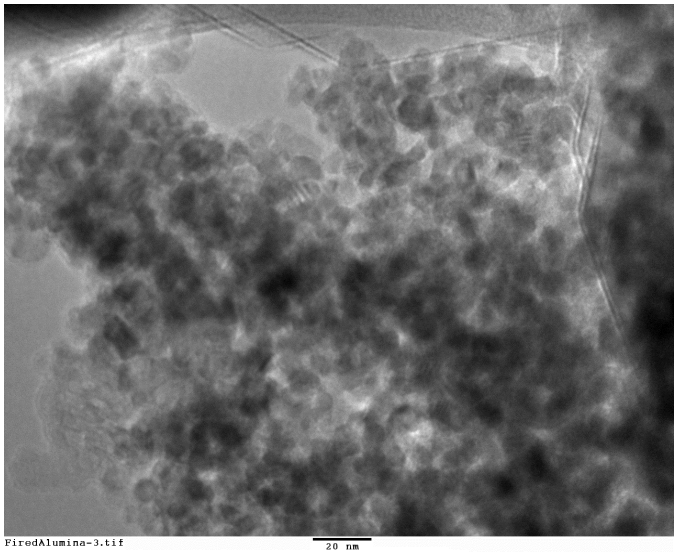

Fig. 12. TEM image of the alumina nanofiber debris (scale bar: 20 nm)

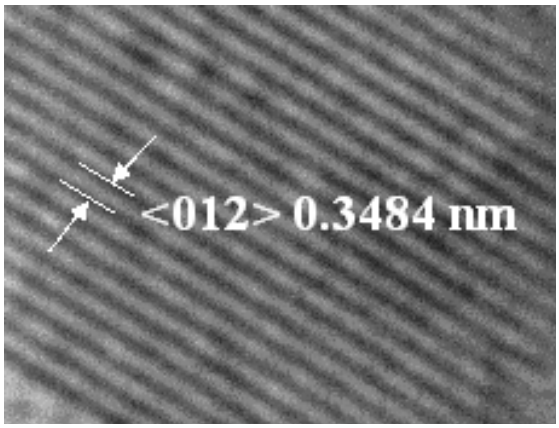

Fig. 13. HRTEM picture of the alumina nanofibers

4. Conclusions

Alumina nanofibers have been synthesized via electrospinning of a polymeric composite solution of aluminum 2, 4-pentanedionate in acetone. The polymeric component (PVP) was used to impart the required viscosity to the inorganic precursor solution. The resulting ceramic-polymer (cermer) composite was calcined in a well-conceived temperature-time-heating rate profile in the range of 1000–1500°C to understand the pathway of phase evolution in the ultimate ceramic product with the scope of retention of the fibrillar artifacts. Analytical tools, such laser Raman spectroscopy, X-ray diffraction, scanning and high resolution transmission electron microscopy in conjunction with energy dispersive X-ray spectroscopy and selected area electron diffraction were employed to carry out systematic structural and microstructural characterization of alumina fibers as a function of heat treatment given to the as-spun material. This investigation showed that α-alumina nanofibers of high structural quality possessing uniform diameter and high aspect ratios could be produced by electrospinning technique.

Acknowledgements. The authors wish to thank Tom Jacob (electronic technician) and Robert Dunmyer (laboratory machinist) for their continued help in various design aspects of this research.

References

[1] J. Zeleny, " The discharge of electricity from pointed conductors differing in size", *Phys. Rev.* 15, 305–333 (1907).

[2] T. Subbiah, G.S. Bhat, R.W. Tock, S. Parameswaran, and S.S. Ramkumar, "Electrospinning of nanofibers", *J. Appl. Polymer Sci.* 96, 557–569 (2005).

[3] I. Chun, *Fine Fibers Spun by Electrospinning Process from Polymer Solutions and Polymer Melts*, Ph.D. Dissertation, University of Akron, 1995.

[4] D.H. Reneker, A.L. Yarin, H. Fong, and S. Koomhongse, "Bending instability of electrically charged liquid jets of polymer solutions in electrospinning", *J. Appl. Phys.* 87, 4531–4547 (2000).

[5] A.G. MacDiarmid, W.E. Jones, I.D. Norris, J. Gao, A.T. Johnson, N.J. Pinto, J. Hone, B. Han, F.K. Ko, H. Okuzaki, and M. Llaguno, "Electrostatically-generated nanofibers of electronic polymers", *Synthetic Metals* 119, 27–30 (2001).

[6] J.-S. Kim and D.H. Reneker, "Mechanical properties of composites using ultrafine electrospun fibers", *Polymer Composites* 20, 124–131 (1999).

[7] D.H. Reneker and I. Chun, "Nanometre diameter fibres of polymer produced by electrospinning", *Nanotechnology* 7, 216–223 (1996).

[8] J.-S. Kim and D.H. Reneker, "Polybenzimidazole nanofiber produced by electrospinning", *Polym. Eng. Sci.* 39, 849–854 (1999).

[9] T.A. Kowalewski S. Blonski, and S. Barral, "Experiments and modeling of electrospinning process", *Bull. Pol. Ac.:Tech.* 53 (4), 385–394 (2005).

[10] Z. Sun, E. Zussman, A.L. Yarin, J.H. Wendorff, and A. Greiner, "Compound core-shell polymer nanofibers by co-electrospinning", *Adv. Mater.* 15, 1929–1932 (2003).

[11] C. Hsu and S. Shivkumar, "Nano-sized beads and porous fiber constructs of poly (ε-caprolactone) produced by electrospinning", *J. Mater. Sci.* 39, 3003–3013 (2004).

[12] C.T. Laurencin and F.K. Frank, *US Patent* 6 (689),166 (2004).

[13] A. Formhals, *US Patent* 1 (975), 504 (1934).

[14] `http://fluid.ippt.gov.pl/sblonski/nanofibres.html`

[15] D. Li and Y. Xia, "Fabrication of titania nanofibers by electrospinning", *Nano Lett.* 3, 555–560 (2003).

[16] D. Li, Y. Wang, and Y. Xia, "Electrospinning nanofibers as uniaxially aligned arrays and layer-by-layer stacked films", *Adv. Mater.* 16, 361–366 (2004).

[17] R. Kessick, J. Fenn, and G. Tepper, "The use of AC potentials in electrospraying and electrospinning processes", *Polymer* 45, 2981–2984 (2004).

[18] Y. Xia and P. Yang, "Guest editorial: Chemistry and physics of nanowires", *Adv. Mater.* 15, 351–352 (2003).

[19] Y. Xia, P. Yang, Y. Sun, Y. Wu, B. Mayers, B. Gates, Y. Yin, F. Kim, and H. Yan, "One-dimensional nanostructures: synthesis, characterization, and applications", *Adv. Mater.* 15, 353–389 (2003).

[20] D. Li and Y. Xia, "Electrospinning of nanofibers: Reinventing the wheel?", *Adv. Mater.* 16, 1151–1170 (2004).

[21] S. Choi, B. Chu, S.G. Lee, S.W. Lee, S.S. Im, S.H. Kim, and J.K. Park, "Titania-doped silica fibers prepared by electrospinning and sol-gel process", *J. Sol-Gel Sci. Technol.* 30, 215–221 (2004).

[22] H. Guan, C. Shao, Y. Liu, N. Yu, and X. Yang, "Fabrication of $NiCO_2O_4$ nanofibers by electrospinning", *Solid State Communications* 131, 107–109 (2004).

[23] M.M. Demir, M.A. Gulgan, Y.Z. Menceloglu, B. Erman, S.S. Abramchuk, E.E. Makhaeva, A.R. Khokhlov, V.G. Mateeva, and M.G. Sulman, "Palladium nanoparticles by electrospinning from poly(acrylonitrile-co-acrylic acid)-$PdCl_2$ solutions. Relations between preparation conditions, particle size, and catalytic activity", *Macromolecules*, 37, 1787–1792 (2004).

[24] W. Sigmund, J. Yuh, H. Park, V. Maneeratana, G. Pyrgiotakis, A. Daga, J. Taylor, and J. Nino, "Processing and structure relationships in electrospinning of ceramic fiber systems", *J. Am. Ceram. Soc.* 89, 395–410 (2006).

[25] J.T. McCann, D. Li, and Y. Xia, "Electrospinning of nanofibers with core-sheath, hollow, or porous structures", *J. Mater. Chem.* 15, 735–738 (2005).

[26] H. Knözinger and P. Ratnasamy, "Catalytic aluminas: surface models and characterization of surface sites", *Catal. Rev. Sci. Eng.* 17, 31–39 (1978).

[27] M. Che and C.O. Bennett, "The influence of particle size on the catalytic properties of supported metals", *Adv. Catal.* 36, 55–63 (1989).

[28] D.J. Eichenberg, NASA Glenn Research Center, Cleveland, `http://www.nasatech.com/Briefs/Nov03/LEW17190.html`

[29] A.-M. Azad, "Fabrication of yttria-stabilized zirconia nanofibers by electrospinning," *Materials Letters*, 60, 67–72 (2006).

[30] A.-M. Azad, T. Matthews, and J. Swary, "Processing and characterization of electrospun Y_2O_3-stabilized ZrO_2 (YSZ) and Gd_2O_3-doped CeO_2 (GDC) nanofibers," *Materials Science and Engineering B* 123, 252–258 (2005).

[31] V. Saraswati, G.V.N. Rao, and G.V. Rama Rao, "Structural evolution in alumina gel", *J. Mater. Sci.* 22, 2529–2534 (1987).

[32] G.V. Rama Rao, S. Venkadesan, and V. Saraswati, "Surface area and pore size studies of alumina gels", *J. Non-Crystalline Solids* 111, 103–112 (1989).

[33] A.C. Ferrari and J. Robertson, "Interpretation of Raman spectra of disordered and amorphous carbon", *Phys. Rev. B* 61, 14095–14107 (2001).

[34] A.C. Ferrari and J. Robertson, "Resonant Raman spectroscopy of disordered, amorphous, and diamond-like carbon", *Phys. Rev. B* 64, 075414 (1)–075414 (13) (2001).

[35] R. Saito, A. Jorio, J. H. Hafner, C. M. Lieber, M. Hunter, T. McClure, G. Dresselhaus and M. S. Dresselhaus, "Chirality-dependent G-band Raman intensity of carbon nanotubes", *Phys. Rev. B* 64, 085312(1)–085312(7) (2001).

[36] C.J. Doss and R. Zallen, "Raman studies of sol-gel alumina: Finite size effects in nanocrystalline AlO(OH)", *Phys. Rev. B* 48, 15626–15637 (1993).

[37] H.D. Ruan, R.L. Frost, and J.T. Kloprogge, "Comparison of Raman spectra in characterizing gibbsite, bayerite, diaspore and boehmite", *J. Raman Spectr.* 32, 745–750 (2001).

[38] A.L. Patterson, "The diffraction of X-rays by small crystalline particles", *Phys. Rev.* 56, 972–977 (1939).

[39] A.L. Patterson, "The Scherrer formula for X-ray particle size determination", *Phys. Rev.* 56, 978–982 (1939).

[40] F.W.C. Boswell, "Precise determination of lattice constants by electron diffraction and variations in the lattice constants of very small crystallites", *Proc. Phys. Soc.* A 64, 465–478 (1951).

[41] B.D. Cullity, *Elements of X-Ray Diffraction*, 2nd ed., Addison-Wesley, New York, 1978.

[42] K. Ishikawa, K. Yoshikawa, and N. Okada, "Size effect on the ferroelectric phase transition in $PbTiO_3$ ultrafine particles", *Phys. Rev. B* 37, 5852–5855 (1988).

[43] F. Zhang, S.W. Chan, J.E. Spanier, E. Apak, Q. Jin, R.D. Robinson, and I.P. Herman, "Cerium oxide nanoparticles: Size-selective formation and structure analysis", *Appl. Phys. Lett.* 80, 127–129 (2002).

[44] H. Dai, J. Gong, H. Kim, and D. Lee, "A novel method for preparing ultra-fine alumina-borate oxide fibres via an electrospinning technique", *Nanotechnology* 13, 674–677 (2002).